Positron transport: The plasma-gas interface[a)]

J. P. Marler,[1,b)] Z. Lj. Petrović,[2] A. Banković,[2] S. Dujko,[2] M. Šuvakov,[2] G. Malović,[2] and S. J. Buckman[3]
[1]*University of Aarhus, Aarhus C DK-8000, Denmark*
[2]*Institute of Physics, P.O. Box 68, 11080 Belgrade, Serbia*
[3]*CAMS, RSPhysSE, Australian National University, Canberra 2600, Australia*

(Received 7 December 2008; accepted 12 January 2009; published online 24 February 2009)

Motivated by an increasing number of applications, new techniques in the analysis of electron transport have been developed over the past 30 years or so, but similar methods had yet to be applied to positrons. Recently, an in-depth look at positron transport in pure argon gas has been performed using a recently established comprehensive set of cross sections and well-established Monte Carlo simulations. The key novelty as compared to electron transport is the effect of positronium formation which changes the number of particles and has a strong energy dependence. This coupled with spatial separation by energy of the positron swarm leads to counterintuitive behavior of some of the transport coefficients. Finally new results in how the presence of an applied magnetic field affects the transport coefficients are presented. © *2009 American Institute of Physics*.
[DOI: 10.1063/1.3078103]

I. INTRODUCTION

Low energy positrons are now used in many fields including atomic physics, material science, and medicine.[1] For most of these applications, well defined, either spatially or energetically, beams are required. Plasma physics provides new tools for this research, including Penning–Malmberg–Surko buffer-gas traps[2] to accumulate positrons and the use of rotating electric fields (the "rotating wall" technique) to compress positrons radially and create tailored beams.[1] More recently, progress in producing high resolution, small diameter beams has been made by locating the Penning–Malmberg trap in a high magnetic field (5 T) superconducting magnet.[3] While this technique results in a greater efficiency of trapped positrons (due to minimized loss of positrons since there is no buffer gas). This technique may not be appropriate for all applications. Primarily those in which it may be undesirable to have a highly magnetized beam or those in which an expensive, large superconducting magnet is not feasible. Finally it seems that even the high-field magnetic trap may require some type of a primary buffer-gas trapping stage before positrons can be trapped in the high field trap. Therefore a part of the motivation for the present work remains to study the dynamics inside the buffer-gas trap.

We may therefore divide the traps into two groups: those where high magnetic fields are used with high vacuum and those where collisions with buffer gas thermalize the positrons. In principle, the latter systems belong to the group of so-called swarm experiments.[4,5] Swarms are ensembles of noninteracting particles whose behavior is determined by the external field and their collisions with the background gas. While in collisional traps conditions are not met where use or determination of well defined averaged quantities known as transport coefficients may be feasible, it is worth noting that well defined swarm experiments for positrons (similar to those for electrons) were built in the past either to measure thermalization times or transport coefficients. (See, for example, Ref. 6 or Ref. 7, a nice review of these experiments is forthcoming, see Ref. 8.) While the thermalization experiments had some degree of success, experiments to measure transport coefficients were never properly developed partly because they were difficult to implement and partly because proper tools for theoretical analysis had not been developed yet.[8]

In this paper we start with a review of recent results for positron transport in gases[9–11] based both on new cross section data and on a new understanding of nonconservative kinetic phenomena for charged particles in gases.[5,12] Although argon is not considered a buffer gas of choice, it does exhibit some of the strongest observed kinetic effects to date, and so this paper starts by using argon as a test gas for describing and examining the new transport phenomena observed. Finally, we present new results from studying the effect of an applied external magnetic field to the system perpendicular to the direction of the electric field.

II. MONTE CARLO SIMULATION AND DEFINITIONS OF TRANSPORT COEFFICIENTS

In this work we apply a Monte Carlo (MC) simulation code that follows a large number of positrons (typically 1×10^5) through a neutral gas under the influence of uniform and crossed electric and magnetic fields. The simulations were performed for the low space charge limit according to the standard definition of charged particle swarms. Under those conditions the results only depend on E/N, although we may note that we have used the pressure of 1 Torr for simulations. A possible breakdown of E/N scaling would occur at pressures so high that scattering on more than one molecule occurs at the same time, i.e., when the mean distance between molecules is smaller than the de Broglie wavelength. Gas temperature was taken to be zero or room

[a)]Paper TI1 6, Bull. Am. Phys. Soc. **53**, 239 (2008).
[b)]Invited speaker.

 © 2009 American Institute of Physics

Author complimentary copy. Redistribution subject to AIP license or copyright, see http://php.aip.org/php/copyright.jsp

temperature, but the difference is insignificant for mean positron energies exceeding 100 meV. It is assumed that the positron swarm develops in an infinite space. Positrons gain energy from the external electric field and dissipate it through the collisional transfer to the neutral gas atoms. Binary elastic, inelastic, and nonconservative collisions are included. The code is also designed to include thermal effects in positron transport as well as superelastic collisions. Our MC simulation technique has been verified for a number of benchmarks for electrons, particularly when nonconservative collisions are operative.[13] Rather than present a full review of the simulation technique, we highlight below some important points associated with the technique and refer the reader to our recently published papers, Refs. 9, 14, and 15, for a detailed discussion.

In the present MC code, we follow the spatiotemporal evolution of each positron through time steps governed by the minimum of the two relevant time constants: mean collision time and cyclotron period. These finite time steps are used to solve the integral equation for the collision probability in order to determine the time of the next collision. Once the moment of the next collision is established, the nature of the collision is determined by using the relative probabilities of the various collision types. All positron scattering is assumed to be isotropic regardless of the collision nature. Transport coefficients are determined after relaxation to the steady state. Given the expected significance of positronium (Ps) formation (described below), transport coefficients were calculated just below and in the region where the Ps formation is significant.

The main transport coefficients considered here are the drift velocities. Historically what was calculated was the flux drift velocity defined through the flux-gradient equations, in this case, Fick's law. It can be calculated from the spatially uniform average velocity. Typically mean velocities are several orders of magnitude smaller than random particle velocities. However, as this only samples the velocity of the remaining particles from the velocity distribution function (velocity space), it does not take into account the fact that particles may be lost or gained from the system at preferential locations which may be generated by spatial separation between slower and faster particles. Therefore, in general, the velocity averaged drift velocity is not a measurable quantity as measurements are performed in configuration space. It is thus useful to consider the so-called bulk drift velocity,[16] where the average is carried out over the configuration space. The two drift velocities, the flux w_F and the bulk drift velocity W_B, are defined as

$$w_F = \langle v_z \rangle \quad \text{flux},$$

$$W_B = d\frac{\langle z \rangle}{dt} \quad \text{bulk}.$$

The two should only be the same if the summation limit in the averaging operator does not depend on time. If the summation limit, which is equal to the number of particles, changes with time, there is a difference between the two properties. Historically, only flux properties were calculated by most scientists and it was not well known that the measured values, the bulk properties, are different in their nature from the calculated flux values.

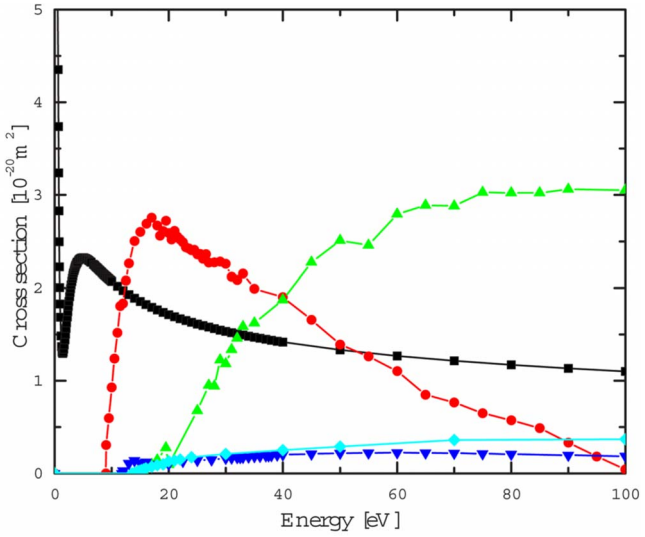

FIG. 1. (Color online) Set of positron scattering from argon cross sections: (squares) total (Refs. 18 and 19); (circles) Ps formation (Ref. 20); (triangles up) ionization (Ref. 20); (triangles down) electronic excitation of the two lowest lying $3p_5 4s$ $J=1$ levels (Refs. 21 and 22); and (diamonds) excitation of higher singlet levels based on that for electron impact excitation of argon (Ref. 23). See Ref. 9 for more details.

III. RESULTS IN ARGON

A complete set of cross sections for positron scattering from argon is shown in Fig. 1. Most important to note is where these cross sections differ from typical electron cross sections. Most striking is the Ps formation channel. Positronium (the temporary bound state of an electron and positron) can be formed from the positron and the ionized electron during ionization of the atom or molecule. The threshold for this process is 6.8 eV, the binding energy of Ps, earlier than the onset of ionization. Direct ionization (i.e., ionization resulting in a free electron and positron) therefore results in a competing process only past its own threshold. It should be noted that direct ionization (unlike the case for electrons) is *not* nonconservative. The result in terms of the Ps formation cross section is a relatively large, sharply energy dependent cross section. As this also results in loss of positrons from the system, this is similar to attachment for electrons but the cross section for Ps formation is typically two orders of magnitude larger and here lies the biggest difference between electron and positron impact. Direct annihilation (i.e., annihilation without first forming positronium) was not considered as it is orders of magnitude smaller than elastic scattering and positronium formation.[17] Thus, the number of events in simulation would be too small to have good statistics. It should be noted that there is no nonconservative multiplication process for positrons which would serve as the analogous process to ionization for electrons. Further explanation of the choice of cross section data is given in Ref. 9.

Figure 2 compares the results of the mean energies for positrons and electrons. In general, one would expect the mean energy of positrons to be higher at the same E/N (the

Author complimentary copy. Redistribution subject to AIP license or copyright, see http://php.aip.org/php/copyright.jsp

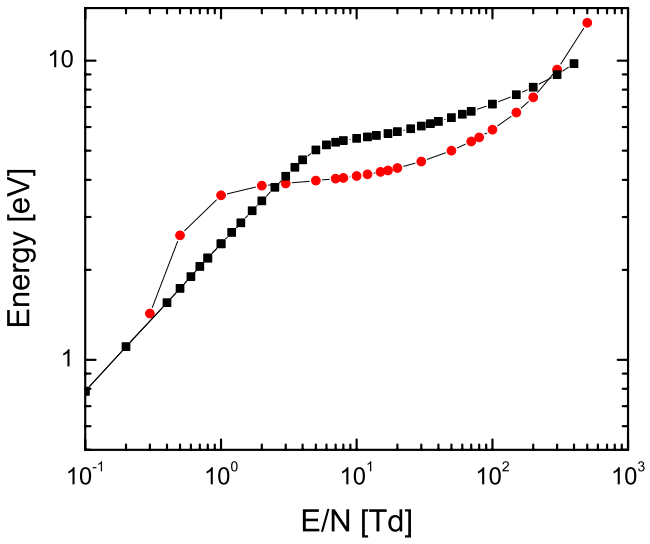

FIG. 2. (Color online) Comparison of positron (circles) and electron (squares) mean energies (Ref. 9).

unit for E/N is Townsend: 1 Td=10^{-21} V m^2) due to a smaller number of available inelastic channels. This is, however, only seen in the range above ~100 Td. At threshold, the Ps formation rate increases sharply with energy, and above the threshold, Ps formation acts to effectively cool the energy distribution function by selectively removing the higher energy positrons. This leads to a lower mean energy of positrons in the E/N range where Ps formation is dominant.

Figure 3 compares the drift velocities for positrons and electrons. In this energy range for electrons in argon, the flux and bulk drift velocities are effectively the same, i.e., where ionization (the only nonconservative process available in that system) is insignificant. Additionally, the electron and positron flux drift velocities have a qualitatively similar dependence on E/N as was expected as nonconservative processes

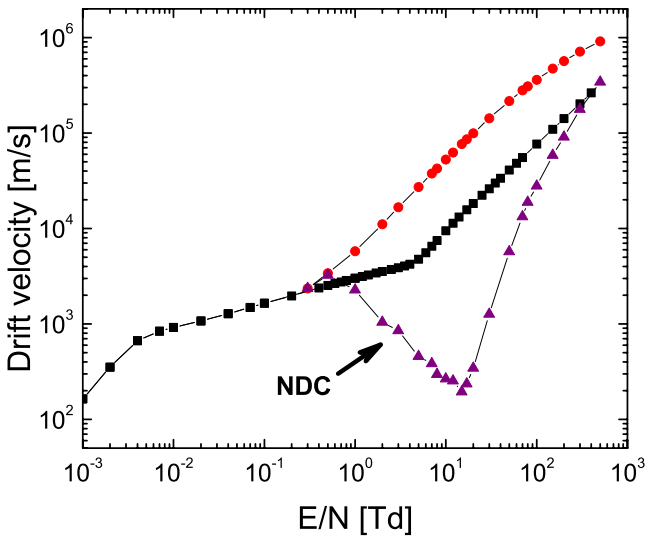

FIG. 3. (Color online) Comparison of positron flux (circles) and bulk (triangles) and electron flux and bulk (squares) drift velocities (Ref. 9). Marked with an arrow is the area of NDC in the bulk drift velocities for positrons.

are not included in the calculation of the flux. On the other hand, looking just at positrons, the flux and bulk drift velocities are markedly different, both qualitatively and quantitatively. Specifically, while the magnitude of the positron flux drift velocity increases monotonically with E/N, the bulk drift velocity decreases with increasing E/N in the range of 1–15 Td and reaches a minimum which is several orders of magnitude below the flux drift velocity at around 15 Td.

This region, 1–15 Td in the bulk drift velocity demonstrates the negative differential conductivity effect (NDC).[24–26] NDC refers to the phenomenon where the mean velocity decreases when E/N is increased. In principle, the conductivity also involves the dependence of the number of particles but the fundamental properties of drift velocities are less trivial and therefore the NDC in practice and in this paper only refers to the drift velocity. The origin of NDC has been explained by a number of authors, and specific criteria have been specified in particular for the case of electrons which depend on the shapes of the elastic and inelastic cross sections.[24–27] More recently the adaptation of these criteria to the case for positrons has been investigated.[10] Note that although the mean velocity decreases when E/N is increased, the mean energy and the mean absolute value of the velocity $\langle|\mathbf{v_i}|\rangle$ increase.

Most importantly there is nothing in our experience with electrons that prepares us for the fact that the flux property shows no signs of NDC, while it is very strongly present in the bulk property. While Vrhovac and Petrović[26] were the first to discuss how the nonconservative nature of collisions may induce NDC, their conclusion, based on the relevant processes for electrons, was the NDC in the bulk may only occur if conditions for NDC in the flux velocity are almost met, i.e., there is a plateau in the flux drift velocity. In the case of argon just by observing the flux drift velocity and the cross sections, one sees that the flux drift velocity is nowhere near the conditions leading to NDC. Thus the observation of the bulk drift velocity NDC was unexpected.

IV. A CLOSER LOOK AT NDC IN ARGON

Perhaps a simple first look into how Ps formation affects NDC in this system is to simulate transport in argon assuming that Ps formation is an inelastic process. The code was modified to include an inelastic process which has the same shape cross section as Ps formation but does not remove a positron from the system only decreases the positron energy by the threshold energy for Ps formation. Figure 4 shows the results from such a simulation. The bulk drift velocity calculated in this way now almost exactly matches the flux drift velocity. This lends credence to the assumption that it is the nonconservative nature of Ps formation which causes the observed NDC in the bulk drift velocity. In other words, it is not in the shape of the Ps formation cross section but in the effect of the number changing nature of the process on the distribution functions.

A second check is to analyze whether the standard formula defining the difference between the bulk and flux properties[28] works well in this case. The formula is

Author complimentary copy. Redistribution subject to AIP license or copyright, see http://php.aip.org/php/copyright.jsp

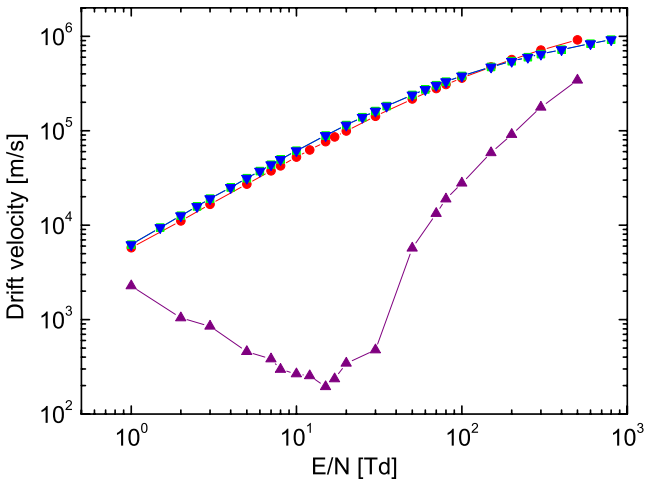

FIG. 4. (Color online) Comparison of positron bulk drift velocity (up triangles) with the bulk drift velocity calculated when Ps formation is treated as an inelastic process (down triangles). Also shown for reference is the positron flux drift velocity (circles) (Ref. 9).

$$W_B = w_F - \frac{2\varepsilon}{3e}\frac{d\nu_{\mathrm{Ps}}}{dE}, \tag{1}$$

where ν_{Ps} is the Ps formation rate, ε is the mean energy, e is the elementary charge, and E is the electric field. Shown in Fig. 5 is a comparison of the MC bulk drift velocity and the right hand side of Eq. (1) found by subtracting the second term found from the MC determined rates of Ps formation from the MC flux drift velocity. There is good agreement with the onset of NDC, although the shapes between the plotted left and right hand sides of Eq. (1) do not match perfectly.

The next thing to investigate is if the calculated drift velocity satisfies the NDC criteria for electrons given in Ref.

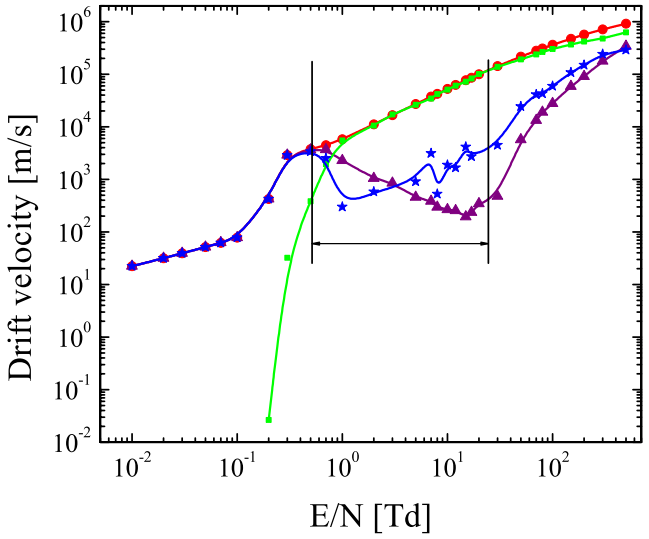

FIG. 5. (Color online) Comparison of positron MC calculated bulk drift velocity (triangles) with the bulk drift velocity as computed by the subtraction indicated in the right hand side of Eq. (1) (stars). Also shown for reference are the MC calculated flux drift velocity (circles) and the second term from the right hand side of Eq. (1) (squares) (Ref. 10). See text for details.

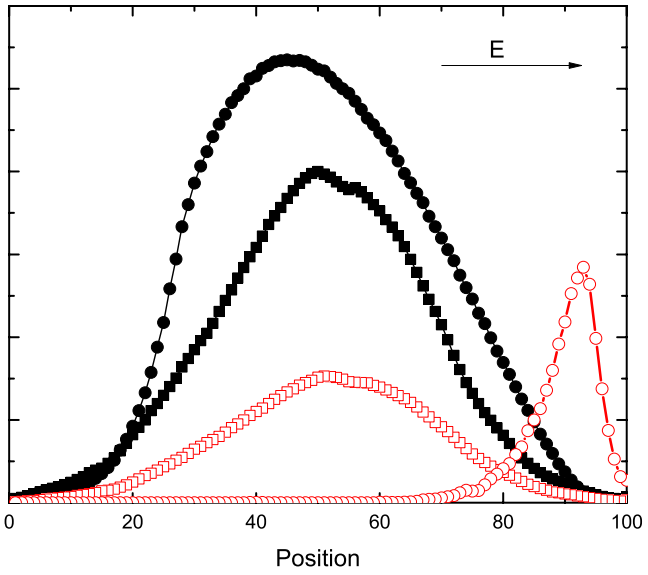

FIG. 6. (Color online) Comparison of spatial profiles (solid) and the location of the positroniums formed (open) as a function of position at 100 Td (squares) and 5 Td (circles) (Ref. 9).

26 but modified for positron transport such that Ps formation takes the role of attachment. The criterion is then given as

$$\frac{dW_B}{dE} = \frac{dw_F}{dE} - \frac{1}{e}\frac{2}{3}\left[\frac{d\varepsilon}{dE}\frac{d\nu_{\mathrm{Ps}}}{dE} + \varepsilon\frac{d^2\nu_{\mathrm{Ps}}}{dE^2}\right] < 0. \tag{2}$$

As shown in Fig. 5, the region where the MC calculated drift velocity falls and the predictions of the criterion (the region between the vertical lines) coincides. The agreement is better for the onset than for the end of the range but overall the qualitatively prediction is good.

The most likely candidate to explain the remaining differences can be seen by looking at the spatial profiles. Figure 6 shows a comparison between the spatial profiles at two different applied external fields: 100 and 5 Td. The spatial profile at 100 Td, which is significantly passed the NDC region, is basically symmetric. At this E/N, the spatial profiles of the mean energy and Ps formation rate show only a weak dependence on the axial position.[10] The mean energy is above the Ps formation threshold, the spatial profile of Ps formation events is symmetric and to a large degree follows the density profile of the swarm.

However at 5 Td, which is in the middle of the NDC region, the spatial profile is significantly different. Instead of being symmetric around $x=50$, the front end (i.e., high energy side) is cut off. This can be understood by looking at the spatial profile of Ps formation events. They are exclusively at the front end of the pulse where the positrons have energy greater than the Ps formation threshold. In summary, positrons that are accelerated by the field reach energies where Ps formation reigns and then they will most likely disappear. In the energy region where Ps formation is the dominant process (with the exception of elastic scattering), positrons disappear before they can gain sufficient energy to be accelerated in the direction of the field.

The extreme skewing of the spatial profile enhances the effect on the bulk velocity as compared to the predictions of

Author complimentary copy. Redistribution subject to AIP license or copyright, see http://php.aip.org/php/copyright.jsp

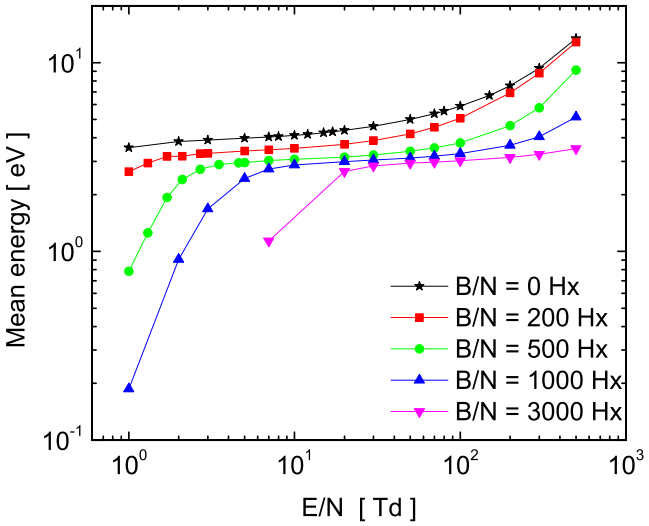

FIG. 7. (Color online) The variation in the mean energy with E/N for various B/N as indicated in the graph.

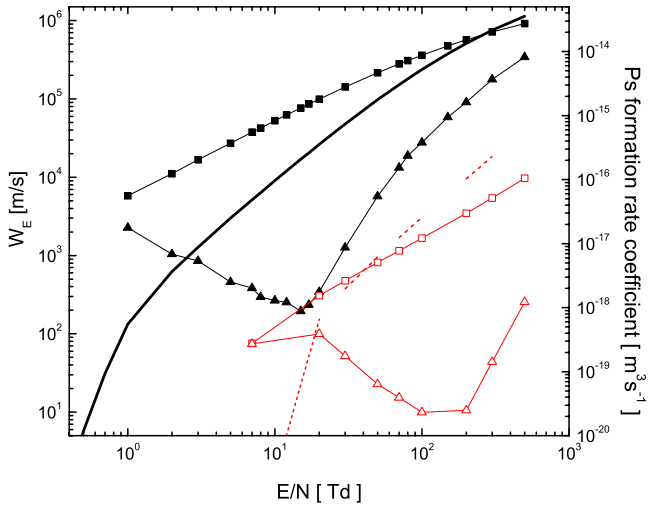

FIG. 8. (Color online) The variation in the flux (squares) and bulk (triangles) drift speed and Ps formation rate with E/N for the $B/N=0$ (solid symbols and line) case and E/N dependence of the longitudinal drift velocity component and Ps formation rate for B/N of 3000 Hx (open symbols and dashed line).

Vrhovac and Petrovic[26] given by Eq. (2). This is due to the fact that the theory was not able to include such spatial profile variations. The theory provides the physical understanding for the observed NDC in bulk drift velocity, but quantitative comparisons should be done with results of simulations that may accommodate arbitrary spatial profiles.

V. POSITRON TRANSPORT IN CROSSED ELECTRIC AND MAGNETIC FIELDS

In this section we present new results on the effects of magnetic field (perpendicular to the electric field) on the positron transport properties in argon. This is not intended to be a comprehensive investigation of positron swarms in electric and magnetic fields in complex geometries found in collisional traps or other possible applications involving magnetic fields. Rather the current aim is to demonstrate the applicability of the present MC code under conditions where the positron transport in electric and magnetic fields is greatly influenced by the Ps formation.

Figure 7 shows the variation in the mean energy with E/N for various B/N. Recall the characteristics of the magnetic field-free case ($B/N=0$ Hx). After the threshold of Ps formation, only a very slow rise in the mean energy and only at the end of the range shown in this plot a steeper rise indicating the reduced influence of the Ps formation and progressive influence of the electronic excitation processes in controlling the energy of the positron swarm. When the magnetic field is applied, the profiles of the mean energy are essentially displaced down and toward higher E/N for an increasing B/N. In general, the mean energy monotonically decreases with B/N for a fixed E/N value. This is a clear sign that the well-known phenomenon of magnetic cooling, previously observed in electron transport, directly carries over to positron swarms. This phenomenon results from an inability of the electric field to pump energy into the system because the positrons change their direction of motion due to the magnetic field. The reader is referred to Refs. 14 and 29–31 where the phenomenon of magnetic cooling was discussed for electrons in a broader context.

The lowering of the mean energy at a given E/N as function of increasing B/N is also seen in the drift velocities. Figure 8 shows the variation in the flux and bulk components of the drift velocity along the direction of electric field (E) for the magnetic field-free case and for B/N of 3000 Hx. The same figure shows the variation in the Ps formation rate with E/N under the same two magnetic field conditions. As expected, the onsets of the bulk NDC and of the Ps formation are coincident.

In magnetic fields a perpendicular velocity component is created by the $E\times B$ force; one may, therefore, separate two components of the drift velocity, a longitudinal drift velocity W_E and a perpendicular drift velocity $W_{E\times B}$, and the total magnitude of the drift velocity, W is then defined as $W^2=W_E^2+W_{ExB}^2$. Surprisingly, the total magnitude of the drift velocity, as in Fig. 9, shows no sign of the NDC even for the same conditions where it was exhibited so strongly in the bulk longitudinal drift velocity W_E. Only in the case for $B/N=200$ Hx, one may observe small but noticeable difference between the bulk and flux W at large E/N. For higher B/N values, the bulk and flux W's are completely overlapped. This coincidence between the bulk and flux total drift velocities simply means that the perpendicular drift velocity W_{ExB} which is normally smaller than the longitudinal component W_E (for small B/N), due to the bulk longitudinal drift velocity NDC, becomes larger and dominates the total drift velocity. In other words, the angle of the total drift velocity shifts to almost 90° with respect to the electric field. When W is mainly determined by $W_{E\times B}$, it is not surprising that there are not large nonconservative effects as there is no variation in the electric field in the perpendicular direction to separate the particles in space.[31]

This example illustrates how dramatic the influence of

Author complimentary copy. Redistribution subject to AIP license or copyright, see http://php.aip.org/php/copyright.jsp

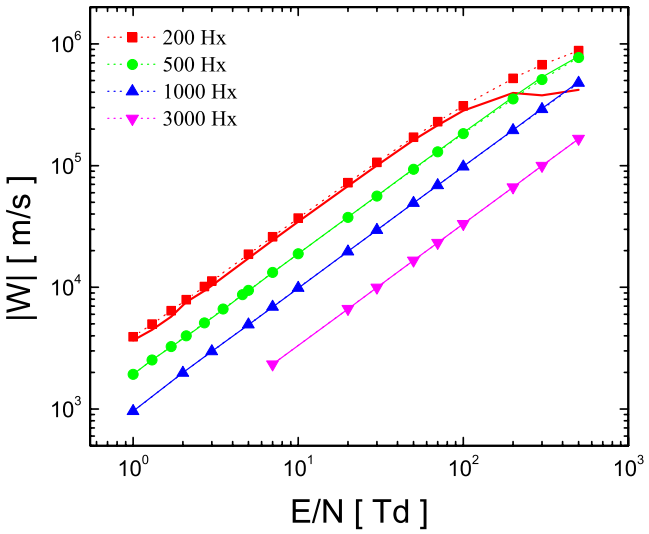

FIG. 9. (Color online) The variation in the flux (full symbols and dotted lines) and bulk (solid lines) drift speed with E/N for various B/N as indicated in the graph.

the magnetic field on positron transport can be. As can be observed, even at $B/N=200$ Hx, the $W_{E\times B}$ dominates W_E. Thus there are two options for the additional control of the NDC effect in electric and magnetic fields. They can be further examined by studying positron transport under conditions of varying angle between the fields. A second option would be to study the effect of a lower B/N than those used here. These studies are ongoing and will be presented in a future paper.

In closing we note that the values of B/N used here are at least three orders of magnitude smaller than those that may be found in collisional (Surko) traps. While this was intentional for these initial investigations, in order to remove all chances of drift across the magnetic lines, the dynamics of particles in collisional trap fields can be represented accurately in our codes. By including a realistic geometry, it would be possible to perform calculations for these systems in an effort to provide a better understanding of these traps and perhaps contribute to their optimization. For the possible swarm (higher pressure) experiments that may be developed in the future these results mean that by varying the magnetic field, it may be possible to move positrons perpendicular and to enable proper time of flight measurements without a large background of nonthermalized positrons.

VI. CONCLUSION

In the present paper we have shown new developments in simulation of transport of positrons in gases. The plethora of kinetic effects found for electrons[5,32] is enriched by a new one that is unique to positrons, the NDC for the bulk drift velocity when there is no such effect for the flux property. The minimum of the drift velocity caused by the NDC is two orders of magnitude smaller than the value without the NDC which is a difference much larger than any observed for electrons. The effect for the drift velocity has been observed experimentally in the past in case of H_2 (Ref. 6) but had not been fully understood. The explanation may now be seen that the bulk drift velocity NDC is due to the nonconservative nature of Ps formation and due to the large magnitude of its cross section. Therefore the condition is met such that the nonconservative term in the definition of the bulk drift velocity begins to dominate and induce the NDC even without proper conditions being met for the flux drift velocity.

Also shown is how the NDC for the bulk property behaves under the influence of an applied perpendicular magnetic field. Specifically that while NDC still exists for the longitudinal drift velocity, the perpendicular drift velocity becomes so large and that it begins to dominate the total drift velocity so much so that no NDC is observed in the magnitude of the total drift velocity.

We hope that the newly observed phenomena will provide sufficient motivation for restarting swarm experiments and for testing these findings. In the mean time, application of such codes for realistic trap geometries and conditions is commencing. Finally we note that it is our hope that these codes may also be modified to describe application of positrons in medicine and materials science if proper modifications are made to describe the collisions in much denser media. A high level of sophistication will be required to verify those codes against very accurate codes or Boltzmann equation theories. (One should note that our predictions in gases have been completely verified by a completely independent technique of numerical solution to the Boltzmann equation, see Ref. 33). If application to biological systems is achieved, it would mean that a number of techniques developed for modeling of low temperature plasmas may be applied to model positron diagnostics and therapy in the living tissue based on accurate binary collision data.

ACKNOWLEDGMENTS

This work was performed under MNTRS Project No. 141025. The authors are grateful to C. Surko, M. Charlton, J. Sullivan, R. Robson, and R. White for discussions, ideas, and collaboration on some of the topics presented here.

[1] C. M. Surko and R. G. Greaves, Phys. Plasmas **11**, 2333 (2004).
[2] S. J. Gilbert, C. Kurz, R. G. Greaves, and C. M. Surko, Appl. Phys. Lett. **70**, 1944 (1997).
[3] J. R. Danielson, T. R. Weber, and C. M. Surko, Phys. Plasmas **13**, 123502 (2006).
[4] T. Makabe and Z. Lj. Petrović, *Plasma Electronics: Applications in Microelectronic Device Fabrication* (CRC, New York, 2006).
[5] Z. Lj. Petrović, M. Šuvakov, Ž. Nikitović, S. Dujko, O. Šašić, J. Jovanović, G. Malović, and V. Stojanović, Plasma Sources Sci. Technol. **16**, S1 (2007).
[6] N. Bose, D. A. L. Paul, and J. S. Tsai, J. Phys. B **14**, L227 (1981).
[7] M. Charlton, J. Phys. B **18**, L667 (1985).
[8] M. Charlton, "Positron transport in gases," J. Phys.: Conf. Ser. (to be published).
[9] M. Šuvakov, Z. Lj. Petrović, J. P. Marler, S. J. Buckman, R. E. Robson, and G. Malović, New J. Phys. **10**, 053034 (2008).
[10] A. Banković, Z. Lj. Petrović, R. E. Robson, J. P. Marler, S. Dujko, and G. Malović, Nucl. Instrum. Methods Phys. Res. B **267**, 350 (2009).
[11] A. Banković, J. P. Marler, M. Šuvakov, G. Malović, and Z. Lj. Petrović, Nucl. Instrum. Methods Phys. Res. B **266**, 462 (2008).
[12] R. D. White, K. F. Ness, and R. E. Robson, Appl. Surf. Sci. **192**, 26 (2002).
[13] Z. Lj. Petrović, Z. M. Raspopović, S. Dujko, and T. Makabe, Appl. Surf. Sci. **192**, 1 (2002).

Author complimentary copy. Redistribution subject to AIP license or copyright, see http://php.aip.org/php/copyright.jsp

[14]S. Dujko, R. D. White, K. F. Ness, Z. Lj. Petrović, and R. E. Robson, J. Phys. D **39**, 4788 (2006).
[15]S. Dujko, R. D. White, and Z. Lj. Petrović, J. Phys. D **41**, 245205 (2008).
[16]R. Robson, Aust. J. Phys. **50**, 577 (1991).
[17]L. D. Barnes, Ph.D. thesis, University of California, 2005.
[18]R. P. McEachran, personal communication (March 1, 2004).
[19]W. E. Kauppila and T. S. Stein, Adv. At., Mol., Opt. Phys. **26**, 1 (1990).
[20]J. P. Marler, J. P. Sullivan, and C. M. Surko, Phys. Rev. A **71**, 022701 (2005).
[21]J. P. Sullivan, J. P. Marler, S. J. Gilbert, S. J. Buckman, and C. M. Surko, Phys. Rev. Lett. **87**, 073201 (2001).
[22]L. A. Parcell, R. P. McEachran, and A. Stauffer, Nucl. Instrum. Methods Phys. Res. B **171**, 113 (2000).
[23]K. Tachibana, Phys. Rev. A **34**, 1007 (1986); A. V. Phelps, http://jilawww.colorado.edu/~avp/collision_data/electronneutral/ELECTRON.TXT
[24]Z. Lj. Petrović, R. W. Crompton, and G. N. Haddad, Aust. J. Phys. **37**, 23 (1984).
[25]R. Robson, Aust. J. Phys. **37**, 35 (1984).
[26]S. B. Vrhovac and Z. Lj. Petrović, Phys. Rev. E **53**, 4012 (1996).
[27]D. Blake and R. E. Robson, J. Phys. Soc. Jpn. **70**, 3556 (2001).
[28]R. Robson, J. Chem. Phys. **85**, 4486 (1986).
[29]K. F. Ness, J. Phys. D **27**, 1848 (1994).
[30]R. D. White, K. F. Ness, and R. E. Robson, J. Phys. D **32**, 1842 (1999).
[31]S. Dujko, Z. M. Raspopović, and Z. Lj. Petrović, J. Phys. D **38**, 2952 (2005).
[32]R. Robson, R. White, and Z. Lj. Petrović, Rev. Mod. Phys. **77**, 1303 (2005).
[33]J. P. Sullivan, S. Buckman, A. Jones, P. Caradonna, C. Makochekanwa, D. Slaughter, Z. Lj.Petrović, A. Banković, J. S. Dujko, and R. White, "Low energy positron interactions: Trapping, transport and scattering," J. Phys.: Conf. Ser. (to be published).

Author complimentary copy. Redistribution subject to AIP license or copyright, see http://php.aip.org/php/copyright.jsp